

# Coral record of reef-water pH across the central Great Barrier Reef, Australia: assessing the influence of river runoff on inshore reefs

J. P. D'Olivo<sup>1,2\*,3</sup>, M. T. McCulloch<sup>1,2</sup>, S. M. Eggins<sup>3</sup>, and J. Trotter<sup>2</sup>

[1] The ARC Centre for Excellence for Coral Reef Studies

[2] School of Earth and Environment, The University of Western Australia, Crawley 6009, Australia

[3] Research School of Earth Sciences, Australian National University, Canberra 0200, Australia

[\*]{current address}

Correspondence to: J. P. D'Olivo ([juan.dolivocordero@uwa.edu.au](mailto:juan.dolivocordero@uwa.edu.au)) and M. T. McCulloch ([malcolm.mcculloch@uwa.edu.au](mailto:malcolm.mcculloch@uwa.edu.au))

## Abstract

The boron isotopic ( $\delta^{11}\text{B}_{\text{carb}}$ ) compositions of long-lived *Porites* coral are used to reconstruct reef-water pH across the central Great Barrier Reef (GBR) and assess the impact of river runoff on inshore reefs. For the period from 1940 to 2009, corals from both inner as well as mid-shelf sites exhibit the same overall decrease in  $\delta^{11}\text{B}_{\text{carb}}$  of  $0.086 \pm 0.033\%$  per decade, equivalent to a decline in seawater pH ( $\text{pH}_{\text{sw}}$ ) of  $\sim 0.017 \pm 0.007$  pH units per decade. This decline is consistent with the long-term effects of ocean acidification based on estimates of  $\text{CO}_2$  uptake by surface waters due to rising atmospheric levels. We also find that, compared to the mid-shelf corals, the  $\delta^{11}\text{B}_{\text{carb}}$  compositions of inner-shelf corals subject to river discharge events have higher and more variable values, and hence higher inferred  $\text{pH}_{\text{sw}}$  values. These higher  $\delta^{11}\text{B}_{\text{carb}}$  values of inner-shelf corals are particularly evident during wet years, despite river waters having lower pH. The main effect of river discharge on reef-water carbonate chemistry thus appears to be from reduced aragonite saturation state and higher nutrients driving increased phytoplankton productivity, resulting in the drawdown of  $\text{pCO}_2$  and increase in  $\text{pH}_{\text{sw}}$ . Increased primary production therefore has the potential to counter the more transient effects of low pH river water ( $\text{pH}_{\text{rw}}$ ) discharged into near-shore environments. Importantly, however, inshore reefs also show a consistent pattern of sharply declining coral

1 growth that coincides with periods of high river discharge. This occurs despite these reefs  
2 having higher  $\text{pH}_{\text{sw}}$ , demonstrating the over-riding importance of local reef-water quality and  
3 reduced aragonite saturation state on coral reef health.

## 4 5 **1 Introduction**

6 Coral reefs are under threat, not only from the global effects of  $\text{CO}_2$  driven climate change  
7 but also from direct local impacts, in particular disturbed river catchments and degraded  
8 water quality (McCulloch et al., 2003; Brodie et al., 2010b). Changing land-use practices  
9 since the arrival of European settlers to the central Queensland region has produced increased  
10 discharge of terrestrial material from the Burdekin River into the Great Barrier Reef (GBR;  
11 McCulloch et al., 2003; Lewis et al., 2007). The increase in discharge of terrestrial material  
12 into the GBR has resulted in a decrease in inshore water quality, mainly through increased  
13 nutrient loads and decreased water clarity (Brodie et al., 2010b; Fabricius et al., 2014). Known  
14 impacts include the promotion of intense and extensive phytoplankton blooms and the  
15 increase in abundance of macro-algae (Devlin and Brodie, 2005; Brodie et al., 2010b).  
16 Changes in water quality within inner-shelf environments of the GBR have also been linked  
17 to a decrease in coral calcification (D'Olivo et al., 2013), coral biodiversity (De'ath and  
18 Fabricius, 2010), decreased coral cover (Sweatman et al., 2011), and crown-of-thorns starfish  
19 outbreaks (Brodie et al., 2005).

20  
21 Despite the mounting evidence for the negative impacts of increased terrestrial discharge into  
22 the GBR, the effect of river flood plumes on the carbonate status of reef waters, a  
23 fundamental property controlling calcification, remains largely unknown. It is commonly  
24 assumed that, because both the salinity and pH of plume waters ( $\text{pH}_{\text{pw}}$ ) are generally much  
25 lower than ocean waters, a decrease in aragonite saturation state ( $\Omega_{\text{arag}}$ ) might be expected  
26 (Salisbury et al., 2008), with consequent negative effects for coastal calcifying organisms  
27 such as corals (e.g. Kleypas, 1999; Doney et al., 2009; McCulloch et al., 2012). The effect of  
28 lower seawater pH ( $\text{pH}_{\text{sw}}$ ) could however be offset by the input of nutrients associated with  
29 river plumes, as in semi-isolated environments (e.g. enclosed lagoons) and/or highly  
30 productive areas where biological processes actively modify the local seawater chemistry  
31 (e.g. Hinga, 2002; Andersson et al., 2005; Bates et al., 2010; Drupp et al., 2011; Falter et al.,  
32 2013; Duarte et al., 2013). For example, increased productivity during phytoplankton blooms

1 can cause  $\text{pH}_{\text{sw}}$  to rise significantly (Hinga, 2002). Nutrient-enhanced photosynthetic activity  
2 has been shown to amplify the seasonal pH cycle by more than 0.5 pH units in experiments  
3 within marine enclosures in Narragansett Bay, Rhode Island (Frithsen et al., 1985), and to  
4 increase  $\text{pH}_{\text{sw}}$  by 0.7 units in the Peruvian coastal upwelling zone (Simpson and Zirino,  
5 1980). In the GBR, it is not known to what extent terrestrial runoff and the associated  
6 phytoplankton blooms influence  $\text{pH}_{\text{sw}}$  and hence coral calcification, partly due to the  
7 sparseness of especially longer-term  $\text{pH}_{\text{sw}}$  and other seawater carbonate system records. To  
8 overcome this, here we use the skeletons of long-lived massive *Porites* corals as archives of  
9 changing environmental conditions. Temporal changes in the boron isotope ( $\delta^{11}\text{B}$ )  
10 composition of the skeletons provide a time series of seawater pH, which together with  
11 instrumental data, help deconvolve the competing impacts of climate, ocean acidification, and  
12 water quality on coral calcification.

13

14 The  $\delta^{11}\text{B}$  composition of biogenic carbonates ( $\delta^{11}\text{B}_{\text{carb}}$ ) is an established paleo-proxy for  
15  $\text{pH}_{\text{sw}}$ , first developed in corals by Vengosh et al. (1991) and Hemming and Hanson (1992)  
16 and more recently refined by Trotter et al. (2011). The method relies on the preferential  
17 incorporation of the isotopically lighter  $\text{B}(\text{OH})_4^-$  over the  $\text{B}(\text{OH})_3$  species into marine  
18 carbonate skeletons, with the relative boron species concentration and isotopic compositions  
19 being pH dependent (Vengosh et al., 1991; Hemming and Hanson, 1992; Hönisch et al., 2004).  
20 Its application to corals has been validated (Hönisch et al., 2004; Reynaud et al., 2004; Trotter  
21 et al., 2011) and used for long-term  $\text{pH}_{\text{sw}}$  reconstructions using massive *Porites* corals  
22 (Pelejero et al., 2005; Liu et al., 2009; Wei et al., 2009; Shinjo et al., 2013). Although coral  
23  $\delta^{11}\text{B}_{\text{carb}}$  compositions closely parallel variations in  $\text{pH}_{\text{sw}}$  (Hönisch et al., 2004; Krief et al.,  
24 2010; Trotter et al., 2011; McCulloch et al., 2012) there is a consistent species-specific  
25 positive offset of coral  $\delta^{11}\text{B}_{\text{carb}}$  compositions above the borate  $\delta^{11}\text{B}$  value for ambient  $\text{pH}_{\text{sw}}$   
26 (Trotter et al., 2011; McCulloch et al., 2012). This elevation of pH was recently shown to be  
27 consistent with the physiological up-regulation of pH at the site of calcification to promote  
28 aragonite precipitation (Trotter et al., 2011; McCulloch et al., 2012). Trotter et al. (2011)  
29 quantified this internal pH offset and consequently derived ambient seawater values based on  
30 the systematic relationships they observed between the measured coral  $\delta^{11}\text{B}_{\text{carb}}$  composition  
31 and  $\text{pH}_{\text{sw}}$ .

32

1 In this study we present annual resolution  $\delta^{11}\text{B}_{\text{carb}}$  data obtained from cores of massive  
2 *Porites* heads collected from two inner-shelf and two mid-shelf reefs of the central GBR  
3 (Figure 1). The  $\delta^{11}\text{B}_{\text{carb}}$  data is used to reconstruct the variability in surface  $\text{pH}_{\text{sw}}$  on annual  
4 timescales for the period from 1940 to 2009. These results are then compared with  
5 measurements of calcification rates (i.e. linear extension) obtained from the same cores,  
6 together with a more extensive database from the central GBR (D'Olivo et al., 2013). This  
7 sampling regime enables comparative analysis of the dynamic inner-shelf reef environments,  
8 which are subject to terrestrial and anthropogenic influences, with the more stable conditions  
9 of mid-shelf reefs that are less exposed to terrestrial runoff and pollutants (Lough,  
10 2001; Furnas, 2003; Brodie et al., 2012). Collectively these coral records of  $\delta^{11}\text{B}$  (this study)  
11 and linear extension (D'Olivo et al., 2013) provide a unique dataset giving insight into the  
12 long-term variability of  $\text{pH}_{\text{sw}}$  in a natural coastal system, and how these changes inter-relate  
13 to other important environmental parameters (temperature, river discharge and nutrient flux)  
14 and their overall influence on coral calcification.

15

## 16 **2 Samples and Methods**

### 17 **2.1 Instrumental river discharge and sea surface temperature records**

18 Monthly records of river water discharge and pH ( $\text{pH}_{\text{rw}}$ ) for both the Burdekin and Herbert  
19 rivers were obtained from the State of Queensland, Department of Environment and Resource  
20 Management (DERM; <http://watermonitoring.derm.qld.gov.au>, 2011). Annual rainfall data is  
21 defined from October to September based on the rainfall seasonal pattern in Queensland, with  
22 October marking the start of the warmer summer wet season (Lough, 2007, 2011). Monthly  
23 sea surface temperature (SST) records were obtained from the Met Office Hadley Centre's  
24 sea ice and sea surface temperature data set, (HadISST1) centred at  $18^\circ\text{ S}$  and  $147^\circ\text{ E}$  with a  
25 spatial resolution of  $1^\circ \times 1^\circ$  (<http://www.metoffice.gov.uk/hadobs/hadisst/>, 2014). Inner-shelf  
26 average monthly in situ SST data for the period from 1993 to 2008 were obtained from the  
27 Australian Institute of Marine Science (AIMS, <http://data.aims.gov.au/>, 2011). The inner-  
28 shelf SST data was derived by averaging temperature logger records at Pandora Reef,  
29 Havannah Island, Cleveland Bay, Pioneer Bay, Cattle Bay, and Pelorous Island (AIMS,  
30 <http://data.aims.gov.au/>, 2011).

## 1 **2.2 Water Samples**

2 Water samples were collected in order to characterize the  $\delta^{11}\text{B}$  composition of the plume  
3 waters ( $\delta^{11}\text{B}_{\text{pw}}$ ) present in the inner-shelf area during flood events, and hence facilitate the  
4 interpretation of the  $\delta^{11}\text{B}_{\text{carb}}$  coral signal. In February 2007, a total of 29 water samples were  
5 collected (by Stephen Lewis, James Cook University) along a northward transect from the  
6 mouth of the Burdekin River to Magnetic Island (Figure 1). In February 2009, a second suite  
7 of water samples were collected (by J.P. D'Olivo) from the Burdekin River bridge, located  
8 between the towns of Ayr and Home Hill, as well as seven seawater samples along a  
9 northward transect from the mouth of the Burdekin River to Pandora Reef. The presence of  
10 discolored water indicated that the river plume had reached all of the sampling sites. After  
11 collection, 125 ml of each sample was filtered through a 0.45  $\mu\text{m}$  Teflon membrane and then  
12 acidified using 2-3 drops of  $\sim 7$  M  $\text{HNO}_3$ . Samples were then stored in acid-cleaned, low-  
13 density polyethylene bottles in a cool room. Salinity data was provided by S. Lewis (2009).  
14 Water samples were analyzed for B by solution quadrupole ICP-MS using a Varian 820 ICP-  
15 MS at the Research School of Earth Sciences at the Australian National University (ANU).  
16  $^{10}\text{Be}$  was used as an internal standard spiked at a concentration of 4 ppb. Water samples were  
17 diluted according to their salinity by 1000 times with respect to a seawater salinity of 35.

18

## 19 **2.3 Sclerochronology and coral sampling for $\delta^{11}\text{B}$ analysis**

20 Five cores were drilled from massive *Porites* coral heads from four sites in the central GBR  
21 (Figure 1): Pandora Reef (PAN02) and Havannah Island (HAV06A and HAV09\_3) from the  
22 inner-shelf, and Rib Reef (RIB09\_3) and Reef 17-065 (1709\_6) from the mid-outer shelf  
23 reefs. All cores exhibit clear and regular annual growth banding. Subsamples representing  
24 annual growth increments, from the beginning of each high density band (for mid-shelf  
25 corals) or luminescent band (for inner-shelf corals), were milled along the axis of maximum  
26 growth of 0.7 cm thick slabs from each core.

27

## 28 **2.4 Boron isotope methodology**

29 The boron isotopic compositions of water samples and annual coral subsamples of cores  
30 HAV06A, PAN02 and RIB03 were analyzed at the ANU by positive thermal ionization mass

1 spectrometry (PTIMS) using a Thermo Finnigan TRITON. Annual coral subsamples of  
2 cores HAV09\_3 and 1709\_6 were analyzed at the University of Western Australia (UWA) by  
3 MC-ICPMS using a NU Plasma II. Prior to analysis, samples were cleaned in H<sub>2</sub>O<sub>2</sub> (for  
4 PTIMS) or in NaOCl (for MC-ICPMS) to remove organic material, then dissolved in HNO<sub>3</sub>,  
5 and the boron then purified using ion chromatography. The boron separation technique used  
6 for the PTIMS is based on methodology by Wei et al. (2009) and refined by Trotter et al.  
7 (2011). For MC-ICPMS, a combined cation/anion ion-exchange technique was employed as  
8 described by McCulloch et al. (2014). In both methods, the boron is collected in relatively  
9 large fractions ensuring 100% collection efficiency. The  $\delta^{11}\text{B}$  composition of water samples  
10 was analyzed by PTIMS following a simplified purification procedure (cf. coral samples) that  
11 omitted the H<sub>2</sub>O<sub>2</sub> cleaning step and employed a single AGW50-X8 cation column elution  
12 followed by an IRA743 column elution (i.e. the final cation column was omitted). The  
13 amount of water sample required to extract and purify 1  $\mu\text{g}$  of B was estimated from the  
14 relationship between the measured [B] and salinity (S) in the flood plume  $B = 0.1299(S) +$   
15  $0.1188$  and  $B = 0.1302(S) - 0.0374$ ; 2007 and 2009, respectively (Figure 2). The amount of  
16 water subjected to the boron extraction and purification procedure varied from 250  $\mu\text{l}$  ( $S =$   
17  $35$ ) to 5,000  $\mu\text{l}$  ( $S = 0.7$ ), while 30,000  $\mu\text{l}$  were processed for the river water sample ( $S = 0$ ).

18

19 All boron isotopic ratios are expressed in the conventional delta notation ( $\delta$ ) relative to the  
20 NBS951 boric acid international standard. Over the course of this study, PTIMS analysis of  
21 the SRM951 standard yielded a mean value of  $\delta^{11}\text{B} = +0.05$  ‰ relative to a reference value  
22 for this standard of 4.054, with an external precision (2 SD) of  $\pm 0.35$  ‰ ( $n = 43$ ) and an  
23 internal precision of  $\pm 0.07$  ‰. Repeated analyses of the samples ( $n = 46$ ) gave an average  
24 reproducibility of  $\pm 0.20$  ‰ (2 SD). A modern coral from Papua New Guinea (NEP B) was  
25 used as a secondary working standard. Repeated NEP B analyses gave an average value of  
26  $26.35 \pm 0.44$  ‰ (2 SD,  $n = 33$ ) using PTIMS, and  $25.96 \pm 0.32$  ‰ (2 SD,  $n = 70$ ) using MC-  
27 ICPMS. The  $\delta^{11}\text{B}_{\text{carb}}$  values of coral samples ( $n = 8$ ) analyzed by PTIMS are consistently  
28 offset by  $+0.45$  ‰ relative to the MC-ICPMS data. To maintain consistency between the two  
29 data sets a  $+0.45$  ‰ correction was therefore applied to the data measured by MC-ICPMS.  
30 Measurements of the international carbonate standards JCP-1 by MC-ICPMS gave a  $\delta^{11}\text{B}$   
31 value of  $24.35 \pm 0.34$  ‰ (2 SD), identical to the  $24.33 \pm 0.11$  ‰ (SE) reported by Foster et al.  
32 (2013) and  $24.22 \pm 0.28$  ‰ (2 SD) reported by Wang et al. (2010).

33

1 Conversion of  $\delta^{11}\text{B}_{\text{carb}}$  to pH of the calcifying fluid ( $\text{pH}_{\text{cf}}$ ) values was undertaken using the  
2 relationship:

$$3 \quad \text{pH}_{\text{cf}} = \text{pK}_{\text{B}} - \log \left[ \frac{\delta^{11}\text{B}_{\text{sw}} - \delta^{11}\text{B}_{\text{carb}}}{\alpha_{\text{B3-B4}} \times \delta^{11}\text{B}_{\text{carb}} - \delta^{11}\text{B}_{\text{sw}} + 1000(\alpha_{\text{B3-B4}} - 1)} \right] \quad (1)$$

4 Where  $\delta^{11}\text{B}_{\text{sw}}$  is the B isotope composition of seawater ( $\delta^{11}\text{B}_{\text{sw}} = 39.61\%$ ; Foster et al., 2010)  
5 and the B isotope fractionation factor ( $\alpha_{\text{B3-B4}}$ ) of 1.0272 is taken from Klochko et al. (2006).  
6 The B dissociation constant ( $\text{pK}_{\text{B}}$ ) was adjusted to the ambient temperature and salinity  
7 (Trotter et al., 2011), the latter especially relevant for corals from the inner-shelf reef region,  
8 which is diluted by fresh water during flood events. Seasonal variation in salinity was  
9 estimated based on the linear relationship observed between the magnitude of past flood  
10 events and corresponding salinity values reported by King et al. (2001) and Walker (1981)  
11 for these reefs (Figure S1).

12

13 Average annual salinity values were estimated using the equation given in Figure S1. For  
14 each year, a dilution factor derived from a two month period of maximum river discharge was  
15 applied to an initial seawater value of 35.5. Despite limitations with this approach, as flood  
16 events are spatially and temporally variable (King et al., 2001; Furnas, 2003), the effect after  
17 correcting the  $\text{pK}_{\text{B}}$  for salinity and temperature on the estimated  $\text{pH}_{\text{sw}}$  value is small ( $< \sim 0.01$   
18 pH units).

19

20 The external  $\text{pH}_{\text{sw}}$  value was estimated following the method for *Porites* sp. as described by  
21 Trotter et al. (2011):

$$22 \quad \text{pH}_{\text{sw}} = (\text{pH}_{\text{cf}} - 5.954)/0.32 \quad (2)$$

23 All measured and reconstructed  $\text{pH}_{\text{sw}}$  values are reported relative to the total pH scale.

24

## 1 **3 Results**

### 2 **3.1 Plume waters boron concentration, $\delta^{11}\text{B}$ ratios and pH during flood** 3 **events**

4 Measured [B] and  $\delta^{11}\text{B}_{\text{pw}}$  are plotted against salinity of the water samples collected during the  
5 flood events of 2007 and 2009 (Figure 2). Salinity ranges from 0 at the river mouth, to 30 at  
6 Havannah Island and 26.5 at Pandora Reef. Salinity and [B] concentration during the flood  
7 events of 2007 and 2009 show a linear relationship ( $r^2 = 0.9834$ ;  $p < 0.0001$ ;  $n = 10$  for 2007  
8 and  $r^2 = 0.9915$ ;  $p < 0.0001$ ;  $n = 8$  for 2009), consistent with conservative mixing of boron  
9 between seawater and flood-waters.

10

11 The flood events sampled in 2007 and 2009 show large differences in the  $\delta^{11}\text{B}_{\text{pw}}$  composition  
12 of the low salinity floodwaters collected close to the river mouth (Figure 2). The low  $\delta^{11}\text{B}_{\text{pw}}$   
13 (+14.13‰) measured during the larger 2009 flood event (29 Teraliters) contrasts with the less  
14 variable and higher  $\delta^{11}\text{B}_{\text{pw}}$  (+42.8‰) of the smaller 2007 flood event (10 Teraliters). River  
15 water collected from the Burdekin River Bridge (23 km upstream from the river mouth)  
16 during the 2009 flood event had a  $\delta^{11}\text{B}_{\text{pw}}$  value of +28‰. Despite the large difference in the  
17  $\delta^{11}\text{B}_{\text{pw}}$  values of waters near the river mouth in the two flood events,  $\delta^{11}\text{B}_{\text{pw}}$  of samples taken  
18 close to the inner-shelf reefs are very similar, with an average  $\delta^{11}\text{B}$  value of  $39.80 \pm 0.34$ ‰ (2  
19 SD;  $n = 2$ ). This value is identical to seawater samples from Lady Musgrave Island in the  
20 southern GBR ( $\delta^{11}\text{B}_{\text{sw}} = 40.09 \pm 0.37$ ‰; 2 SD.;  $n = 2$ ), and is consistent with previously  
21 reported seawater values (Foster et al., 2010).

22

### 23 **3.2 Coral $\delta^{11}\text{B}$ records**

#### 24 **3.2.1 Interannual variability**

25 Coral  $\delta^{11}\text{B}_{\text{carb}}$  compositions for fives cores give average values that range from  $23.6 \pm 0.37$ ‰  
26 to  $25.2 \pm 0.57$ ‰ over the common period of 1973 to 2002 (Table 2). These values are  
27 consistent with previously reported values for *Porites* corals (Hönisch et al., 2004; Pelejero et  
28 al., 2005; Wei et al., 2009; Krief et al., 2010). Using Eq. (1) and Eq. (2), these  $\delta^{11}\text{B}$  values  
29 translate to  $\text{pH}_{\text{sw}}$  values of  $7.88 \pm 0.07$  to  $8.19 \pm 0.11$  (Table 2). The mid-shelf corals have  
30 slightly lower  $\delta^{11}\text{B}_{\text{carb}}$  (and pH) values that are less variable ( $\pm 0.37$  to  $\pm 0.44$ ‰; 2 SD) than the



1 inner-shelf corals, ( $\pm 0.50$  to  $\pm 0.66\%$ ; 2 SD). Differences in  $\delta^{11}\text{B}_{\text{carb}}$  compositions between  
 2 coral cores are significant (Kruskal-Wallis one way ANOVA on ranks). Pairwise multiple  
 3 comparison procedures (Tukey Test;  $p < 0.05$ ) indicate that these differences are significant  
 4 between the three inner-shelf cores and the mid-shelf core 1709\_6; mid-shelf core RIB09\_3  
 5 is only significantly different from inner-shelf core HAV06A. No significant correlation was  
 6 found between the different  $\delta^{11}\text{B}_{\text{carb}}$  coral records.

7

8 Linear regressions applied to the reconstructed annual  $\text{pH}_{\text{sw}}$  time-series for all five coral  
 9 records show a decrease in time over the full length of each coral record (Figure 3). The  
 10 decrease in  $\text{pH}_{\text{sw}}$  is equivalent to  $-0.017 \pm 0.008$  units per decade for the inner-shelf corals and  
 11  $-0.018 \pm 0.007$  units per decade for the mid-shelf corals. These rates are consistent with global  
 12 estimates of 0.017 to 0.019 pH units decrease per decade from 1984 to 2011 based on  
 13 instrumental data (Dore et al., 2009; Santana-Casiano et al., 2007; Bates et al., 2012), but are  
 14 lower than the  $0.041 \pm 0.017$  pH unit decrease per decade for the period of 1940 to 2004  
 15 shown by the  $\delta^{11}\text{B}_{\text{carb}}$  coral record from Arlington Reef (mid-reef) in the Central GBR  
 16 previously reported by Wei et al. (2009). However, the Arlington Reef core exhibited a  
 17 marked decrease in  $\delta^{11}\text{B}_{\text{carb}}$  composition in association with the effects of the severe 1998  
 18 bleaching event.

19

20 Composite records for  $\delta^{11}\text{B}_{\text{carb}}$  were obtained for the inner-shelf and mid-shelf corals (Figure  
 21 4) for the periods of 1963 to 2005 and 1973 to 2009 respectively. These are the periods  
 22 common to more than one core for each region. The data from each core was first normalized  
 23 according to the following equation:

$$24 \quad z_t = x_t - \bar{x}_c \quad (3)$$

25 where  $x_t$  is a  $\delta^{11}\text{B}_{\text{carb}}$  value at a certain point in time,  $\bar{x}_c$  is the mean  $\delta^{11}\text{B}_{\text{carb}}$  value for a given  
 26 coral. The composite records were then obtained by calculating the average from the  
 27 normalized data at a certain point in time. To preserve the units, the composite records were  
 28 ‘re-scaled’ according to the equation:

$$29 \quad r_t = \frac{\bar{z}_t}{\bar{x}_R} \quad (4)$$

1 where  $Z_t$  is a composite  $\delta^{11}\text{B}_{\text{carb}}$  value at a certain point in time,  $\overline{x_R}$  is the average mean  
2 value for all the cores from a specific region. The  $\delta^{11}\text{B}_{\text{carb}}$  annual composite for inner-shelf  
3 and mid-shelf records are plotted relative to time and compared with annual discharge from  
4 the Burdekin River, SST, from HadISST1, as well as coral linear extension rates from  
5 D'Olivo et al. (2013; Figure 4). The composite  $\delta^{11}\text{B}_{\text{carb}}$  records for inner-shelf corals show  
6 significant correlation with river discharge, SST, and coral extension rates (Table 3). The  
7 mid-shelf record shows a weaker but still significant correlation with SST.

8

9 The 8 year low pass filter applied to the composite reconstructed  $\text{pH}_{\text{sw}}$  data derived from the  
10 three inner-shelf  $\delta^{11}\text{B}_{\text{carb}}$  coral records reveals semi-decadal variation (Figure 5), which is not  
11 observed in the mid-shelf  $\delta^{11}\text{B}_{\text{carb}}$  data. Similar variability is observed in inner-shelf coral  
12 extension rates and calcification when periods of slower growth coincide with higher  
13 terrestrial runoff (D'Olivo et al., 2013). It follows that for inner-shelf corals higher  $\delta^{11}\text{B}_{\text{carb}}$   
14 (higher pH) signals coincide with periods of increased river discharge and slower extension  
15 rates.

16

## 17 **4 Discussion**

### 18 **4.1 Variations in river and seawater $\delta^{11}\text{B}$ during flood events**

19 The data from DERM (2011) show that the Burdekin River has an average  $\text{pH}_{\text{rw}}$  of  $7.58 \pm 0.46$   
20 (2 SD; Figure S2); this indicates that low pH fresh water, relative to  $\text{pH}_{\text{sw}}$ , is introduced into  
21 the coastal area of the GBR during wet periods. The  $\text{pH}_{\text{rw}}$  shows no significant difference  
22 between summer ( $7.56 \pm 0.41$ ; 2 SD) and winter ( $7.65 \pm 0.35$ ; 2 SD) values, with a decrease in  
23 pH during some high discharge events, but there is no consistent seasonal pattern. The  
24 variability in  $\text{pH}_{\text{rw}}$  indicates that factors other than the amount of discharge or rainfall  
25 determine the  $\text{pH}_{\text{rw}}$ , and may reflect variability that is related to the nature of the material  
26 being carried by the river and the catchment supplying the water. The  $\delta^{11}\text{B}_{\text{pw}}$  near the mouth  
27 of the Burdekin River can vary significantly between different flood events (Figure 2). Given  
28 that the  $\delta^{11}\text{B}_{\text{rw}}$  is likely influenced by various factors, including both the type and amount of  
29 terrigenous material carried by the river during flood events as well as the source of the river  
30 runoff and nature of the catchment, more work is needed to characterize B dynamics and  
31 isotope fractionation mechanisms during flood events. Although the  $\delta^{11}\text{B}_{\text{pw}}$  values during

1 2007 and 2009 show a large variation close to the Burdekin River mouth, the  $\delta^{11}\text{B}_{\text{pw}}$  values  
2 near the inner-shelf reefs are typical of ocean waters (i.e.  $\delta^{11}\text{B} \sim 40\text{‰}$ ).

3

#### 4 **4.2 Origin of interannual $\delta^{11}\text{B}_{\text{carb}}$ variability in corals**

5 The results shown in Figure 4 and corresponding correlations suggest a relationship between  
6 coral  $\delta^{11}\text{B}_{\text{carb}}$  and both ambient seawater temperature and terrestrial runoff, particularly for  
7 the inner-shelf region of the GBR. However, the interannual  $\text{pH}_{\text{sw}}$  variability of less than  
8  $\pm 0.01$  pH units, which is directly attributable to temperature and salinity changes due to river  
9 run-off, contrasts with the interannual variability of more than  $\pm 0.07$  pH units reconstructed  
10 from the  $\delta^{11}\text{B}_{\text{carb}}$  compositions for the inner-shelf and mid-shelf corals. Possible explanations  
11 for the interannual variability observed in  $\delta^{11}\text{B}_{\text{carb}}$  (reconstructed  $\text{pH}_{\text{sw}}$ ) are examined below.

12

##### 13 **4.2.1 Boron adsorption onto clays and sediments**

14 The interannual  $\delta^{11}\text{B}_{\text{carb}}$  variations for inner-shelf corals could be explained by the adsorption  
15 of B onto sediments and clays that are delivered to the inner-shelf region by rivers. Clays  
16 preferentially remove the lighter isotope  $^{10}\text{B}$  from seawater (Palmer et al., 1987; Barth, 1998).  
17 This selective removal results in the respective depletion of  $^{11}\text{B}$  in marine clays but  
18 enrichment in seawater, and is the accepted explanation for the heavy isotopic composition of  
19 seawater (e.g.  $39.61 \pm 0.04\text{‰}$ ; Foster et al., 2010) relative to average continental crust  
20 (Spivack and Edmond, 1986; Palmer et al., 1987; Barth, 1998). Given the large silt and clay  
21 wash load transported from the Burdekin River (Belperio, 1979), fractionation of  $\delta^{11}\text{B}$   
22 between the dissolved and adsorbed B phases could have a significant effect on the  $\delta^{11}\text{B}$  of  
23 seawater. However, the conservative mixing of B along the transect (Figure 2) indicates that  
24 boron is not being quantitatively removed from the plume waters by clays, and that the clay  
25 material is already in equilibrium with the river water before entering the ocean. Similar  
26 results have been reported by Barth (1998) and Xiao et al. (2007). Furthermore, the oceanic  
27  $\delta^{11}\text{B}_{\text{pw}}$  values near the reefs during flood events and the low B concentration of river waters  
28 require that, at the reef sites, the  $\delta^{11}\text{B}$  signal is dominated by seawater. Finally, large  $\delta^{11}\text{B}_{\text{carb}}$   
29 interannual variations occur on the mid-shelf reefs where there is no clay-dominated  
30 terrestrial runoff.

31

#### 1 4.2.2 Effect of nutrient enrichment and biological productivity on $pH_{sw}$

2 River discharge is an important source of particulate and dissolved nutrients as well as  
3 sediments to the inner-shelf area of the GBR (King et al., 2002; Devlin and Brodie, 2005),  
4 being responsible for ~90% of the particulate and dissolved nutrients introduced during flood  
5 events (Mitchell and Bramley, 1997; Furnas, 2003). Most particulate matter and sediments are  
6 deposited within a few kilometers (~10 km) of river mouths where salinity is <10 (Wolanski  
7 and Jones, 1981), whereas dissolved nutrients are carried greater distances of up to ~200 km  
8 along the coast (Devlin and Brodie, 2005). Once the turbidity decreases and low light levels  
9 are no longer limiting, the dissolved nutrients are rapidly taken up by primary producers  
10 resulting in phytoplankton blooms (Furnas, 2003; Devlin and Brodie, 2005; Brodie et al.,  
11 2010b). These blooms do not usually develop until the salinity reaches ~25, typically  
12 between 50 and 200 km from the river mouth (Devlin and Brodie, 2005) which is where the  
13 inner-shelf coral reefs of this study are located.

14

15 Considering  $NO_3^-$  as the main form of nitrogen sourced from the Burdekin River into the  
16 inner-shelf area of the GBR (Furnas, 2003), plankton productivity will result in the decrease  
17 of seawater  $CO_2$ , increase in alkalinity, and uptake of  $H^+$  (Gattuso et al., 1999). The strong  
18 coupling between  $CO_2$  dynamics and large phytoplankton bloom events observed at  
19 Kane'ohe Bay, Hawaii, changes the reef system from being a source of  $CO_2$  to a sink of  $CO_2$   
20 (Drupp et al., 2011). At Kane'ohe Bay, bloom events are fueled by nutrient inputs following  
21 rainfall and terrestrial runoff events. The enhanced productivity is reflected by increased  
22 phytoplankton biomass from ~2 to ~6  $\mu g\ l^{-1}$  Chl-a, which draws down  $pCO_2$  by ~100 ppm  
23 (Drupp et al., 2011). Similar large nutrient-fueled changes in phytoplankton biomass occur in  
24 the central GBR, where Chl-a increases from between 0.3 and 0.7  $\mu g\ l^{-1}$  Chl-a (Brodie et al.,  
25 2007) to up 1 to 20  $\mu g\ l^{-1}$  Chl-a within flood plumes (Devlin and Brodie, 2005; Brodie et al.,  
26 2010a). For rivers in the central GBR, including the Burdekin, typical DIN (chiefly  $NO_3^-$ )  
27 concentrations during flood conditions vary between 20 and 70  $\mu M$ , while DIP varies  
28 between 0.15 and 1.3  $\mu M$  (Furnas, 2003). These are much higher than typical seawater  
29 concentrations of 0.02  $\mu M$  for DIP and 0.03  $\mu M$  for  $NO_3^-$  during non-flood periods in the  
30 inshore region of the central GBR (Furnas et al., 2011).

31

1 The uptake of CO<sub>2</sub> from nutrient-enhanced productivity and the associated changes to the  
2 carbonate parameters during flood events in the central GBR were estimated using Redfield  
3 ratios and river flood plume nutrient loads (Figure 6). For these calculations we assumed a  
4 conservative dilution process (Wooldridge et al., 2006). Three scenarios are included: in the  
5 first scenario only the changes due to the mixing of plume waters with seawater are  
6 considered (Figure 6a). In the second scenario the input of nutrients from plume waters is  
7 included, with N assumed as the limiting nutrient (Figure 6b). This scenario is consistent with  
8 observations in the GBR where N appears to be the dominant control for new phytoplankton  
9 biomass formation (Furnas et al., 2005). For the final scenario P is considered the limiting  
10 nutrient (Figure 6c). When the effect of nutrient-enhanced productivity is not included  
11 (Figure 6a) there is a small increase in pH<sub>sw</sub> of up to 0.03 units under the most extreme flood  
12 conditions (e.g. salinity 24 near the reef). The scenarios with nutrient input from floodwaters  
13 in figures 6b and 6c result in a more marked increase in pH<sub>sw</sub> due to the drawdown of pCO<sub>2</sub>  
14 associated with nutrient-enhanced productivity. In the case of the scenario with a salinity of  
15 24 and DIN concentration of 23 μM there is a drawdown of pCO<sub>2</sub> of up to 300 ppm and a  
16 corresponding increase in pH<sub>sw</sub> of ~0.33 units (Figure 6b). It follows that the higher δ<sup>11</sup>B<sub>carb</sub>  
17 (and reconstructed pH<sub>sw</sub>) values from the inner-shelf reefs during periods of high river  
18 discharge and high nutrient input are consistent with decreased pCO<sub>2</sub> and increased pH<sub>sw</sub> due  
19 to the stimulation of phytoplankton production.

20

21 In addition to the changes in pH<sub>sw</sub> there is a decrease in Ω<sub>arag</sub>, under the flood scenario with no  
22 nutrient input (Figure 6a), which is associated with the low TA and DIC content of the  
23 floodwaters. The decrease in Ω<sub>arag</sub> can be of up to one unit under extreme flood conditions  
24 (e.g. salinity 24). When nutrient-enhanced productivity is included, the negative effect from  
25 the plume waters on the Ω<sub>arag</sub> is reduced (compare figures 6a with 6b and 6c) as the CO<sub>2</sub>  
26 uptake by the phytoplankton results in an increase in CO<sub>3</sub><sup>2-</sup>. Under the scenario with the  
27 highest DIN concentration (23 μM), the effect from the enhanced productive is sufficient to  
28 counteract the dilution effect in Ω<sub>arag</sub> resulting in a net increase of up to 0.6 units (Figure b).  
29 However, the reduction in Ω<sub>arag</sub> that is expected under most flood conditions is likely to  
30 negatively affect coral calcification (McCulloch et al., 2012). One limitation for the present  
31 model is that it does not allow for air-sea equilibration, which is likely to reduce the effects  
32 from the enhanced productivity on the carbonate parameters.

1

### 2 4.2.3 Cross-shelf differences in coral $\delta^{11}\text{B}_{\text{carb}}$ and reconstructed $\text{pH}_{\text{sw}}$

3 A systematic cross-shelf pattern is observed in  $\delta^{11}\text{B}_{\text{carb}}$  (and reconstructed  $\text{pH}_{\text{sw}}$ ) with both  
4 average values and interannual variability being greater for inner-shelf corals compared to  
5 mid-shelf corals (Table 2). This cross-shelf pattern is consistent with the available, yet  
6 limited,  $\text{pH}_{\text{sw}}$  data that comprises summer (2007) values of  $8.14 \pm 0.003$  (Gagliano et al.,  
7 2010) measured at Magnetic Island in the inner-shelf area, and summer 2012 values of  $8.03$   
8  $\pm 0.03$  measured at Davies Reef (Albright et al., 2013).

9

10 It is not surprising to find differences in reconstructed  $\text{pH}_{\text{sw}}$  values between reefs given that  
11 the GBR is characterized by significant spatial gradients in seawater parameters (e.g.  
12 temperature and water quality), especially across different shelfal environments (D'Olivo et  
13 al., 2013; Cantin and Lough, 2014; Fabricius et al., 2014). These spatial differences could, for  
14 example, account for the lower interannual variation of the coral  $\delta^{11}\text{B}_{\text{carb}}$  records from the  
15 mid-shelf reefs compared to inner-shelf reefs, through the decreased influence of river runoff  
16 on mid-shelf reefs as previously suggested by Wei et al. (2009).

17

18 The reason for the lack of correlation between the  $\delta^{11}\text{B}_{\text{carb}}$  records at nearby reefs, specifically  
19 between Pandora and Havannah Island, is unclear. Differences in biological driven effects  
20 (e.g. species or gender related) or local variability in environmental parameters (e.g. light  
21 regime) are possible explanations. Nevertheless, the overall good agreement between the  
22 composite  $\delta^{11}\text{B}_{\text{carb}}$  coral record and the terrestrial runoff indices is encouraging, suggesting  
23 that multi-core replication (Lough, 2004; Jones et al., 2009) and consideration of ambient  
24 environmental conditions are essential when interpreting  $\delta^{11}\text{B}_{\text{carb}}$  records. Further analyses of  
25 additional records from the same area should help clarify the uncertainties and improve our  
26 understanding of the  $\delta^{11}\text{B}_{\text{carb}}$  seawater proxy in dynamic reefal systems that characterise  
27 inshore environments. A multi-proxy approach should also prove helpful to confirm the  
28 results from this study, but also to determine the response of corals to specific environmental  
29 parameters such as SST, nutrients, sediment or  $\text{pH}_{\text{sw}}$ .

30

#### 1 4.2.4 Relationship between $\delta^{11}\text{B}_{\text{carb}}$ (reconstructed $\text{pH}_{\text{sw}}$ ) and coral growth rates

2 Calcification and linear extension rates of inner-shelf corals from the GBR show a long-term  
3 decrease from the period of 1930 to 2008 (Lough, 2008;D’Olivo et al., 2013). The decrease  
4 in coral growth has been attributed to factors ranging from thermal stress, bleaching,  
5 eutrophication, and ocean acidification (Cooper et al., 2008;Lough, 2008;De’ath et al.,  
6 2009;D’Olivo et al., 2013). The present study reveals that decadal-scale wet periods with  
7 increased terrestrial runoff in the central GBR coincide with periods of reduced inner-shelf  
8 coral growth (Figure 5). The decrease in coral growth occurs despite higher ambient  $\text{pH}_{\text{sw}}$ , as  
9 determined from  $\delta^{11}\text{B}_{\text{carb}}$ . Given the apparently more favorable  $\text{pH}_{\text{sw}}$  for coral growth during  
10 wet periods, other factors such as degraded water quality or reduced  $\Omega_{\text{arag}}$  must clearly be  
11 responsible for the decline in extension rates observed during wet periods. For example,  
12 nutrient-fueled increase in phytoplankton biomass has been a longstanding explanation for  
13 the drowning of coral reefs throughout the geological record (Hallock and Schlager, 1986).  
14 More in situ monitoring of seawater carbonate system parameters (e.g. Uthicke et al., 2014),  
15 especially during wet periods, would greatly help understand the response of the complex  
16 inner-shelf systems to changes in water quality.

17

#### 18 4.2.5 Physiological controls on coral calcification

19 The coral  $\text{pH}_{\text{cf}}$  values calculated from the measured  $\delta^{11}\text{B}_{\text{carb}}$  compositions (Table 2) indicate  
20 that corals elevate the pH at the site of calcification, in agreement with previous studies (Al-  
21 Horani et al., 2003;Venn et al., 2011;McCulloch et al., 2012). This elevation of  $\text{pH}_{\text{cf}}$  for  
22 massive *Porites* grown in the natural environment is estimated to be  $0.41 \pm 0.02$  for the inner-  
23 shelf corals and  $0.43 \pm 0.03$  for the mid-shelf corals. The latter values were estimated using  
24 the coral  $\text{pH}_{\text{cf}}$  values in Table 2 and the directly measured  $\text{pH}_{\text{sw}}$  summer value of 8.14 from  
25 Gagliano et al. (2010) as an independent reference value for the inner-shelf region, and an  
26 average  $\text{pH}_{\text{sw}}$  annual value of 8.06 from Albright et al. (2013) for the mid-shelf region.

27

28 Aside from pH up-regulation at the calcification site (McCulloch et al., 2012), other  
29 processes involved in promoting aragonite precipitation include the transport of ions to the  
30 mineralization site and the synthesis of an organic matrix (Allemand et al., 2004;Venn et al.,  
31 2011). Inhibition or reduced activity of these processes has been associated with significant  
32 reduction of calcification in other studies (Tambutte et al., 1996;Allemand et al., 1998;Al-

1 Horani et al., 2003;Allemand et al., 2004). The reduction in growth of inner-shelf coral may  
2 thus be explained by the effects of river discharge that likely include a decrease in  $\Omega_{\text{arag}}$  that  
3 is accompanied by an increase in shading, turbidity, sedimentation, or competition for carbon  
4 from the photosynthetic activity of zooxanthellae. These factors can affect the availability of  
5 DIC, enzyme activity or synthesis of the organic matrix involved in the calcification process  
6 (Tambutte et al., 1996;Allemand et al., 1998;Al-Horani et al., 2003;Allemand et al., 2004),  
7 because energy and DIC required by these processes is reallocated into cleaning or mucus  
8 production (Riegl and Branch, 1995;Telesnicki and Goldberg, 1995;Philipp and Fabricius,  
9 2003). Therefore, it should not be surprising to find reduced growth during wet periods and  
10 hence degraded water quality despite conditions of higher pH. Critically, this demonstrates  
11 the over-riding importance of local reef water quality relative to the sub-ordinate longer-term  
12 effects of ocean acidification.

13

14 In contrast to the inner-shelf reefs, the  $\delta^{11}\text{B}_{\text{carb}}$  record of the mid-shelf corals shows no  
15 significant relationship to river discharge, consistent with the reduced effects of river flood  
16 plumes. Extreme flood events can however occasionally reach the mid-shelf reefs, especially  
17 when offshore winds occur (King et al., 2002). The presence of subdued luminescent bands  
18 in coral records from Rib Reef that coincide with some large river discharge events, confirm  
19 the minor effect of flood events in the mid-shelf region. Nevertheless, coral linear extension  
20 and calcification at both mid-shelf and outer-shelf reefs increase over the last ~50 years,  
21 coincident with the rise in temperature over this period (D'Olivo et al., 2013). This observed  
22 increase in coral calcification, despite the decrease in the reconstructed  $\text{pH}_{\text{sw}}$ , indicates that  
23 ocean acidification has so far played a secondary role in impacting coral calcification in the  
24 mid-shelf region.

25

## 26 **5 Summary and conclusions**

27 Coral  $\delta^{11}\text{B}_{\text{carb}}$  values show cross-shelf variability with higher average and amplitude values  
28 characteristic of the corals closer to the coast. The reconstructed  $\text{pH}_{\text{sw}}$  values calculated from  
29 the coral  $\delta^{11}\text{B}_{\text{carb}}$  indicate that, in their natural environment, massive *Porites* up-regulate  $\text{pH}_{\text{cf}}$   
30 by ~0.4 units. Variability in coral  $\delta^{11}\text{B}_{\text{carb}}$  show an interannual range in reconstructed  $\text{pH}_{\text{sw}}$   
31 from ~0.07 pH units in mid-shelf corals to ~0.11 pH units in inner-shelf corals, compared to a  
32 much smaller long term (1940 to 2009) trend of ~0.017 pH unit decrease per decade. This



1 rate of change is consistent with previous estimates of decreasing surface  $\text{pH}_{\text{sw}}$  from  $\text{pCO}_2$   
2 driven ocean acidification. Results from  $\delta^{11}\text{B}_{\text{carb}}$  and coral growth indicate that terrestrial  
3 runoff has a significant effect on inner-shelf reef environments. We propose that  
4 phytoplankton blooms, fueled by increased nutrient inputs from river plume waters, drive the  
5 drawdown of dissolved  $\text{CO}_2$  and thus increase the pH in surface seawaters. Consequently, on  
6 a local-scale the inner-shelf reefs of the GBR exhibit high rates of nutrient driven production,  
7 and following river discharge events temporarily counter the effects of ocean acidification.  
8 Despite the higher  $\text{pH}_{\text{sw}}$  we observe an associated decrease in coral linear extension and  
9 calcification (D'Olivo et al., 2013), consistent with expectations where coral calcification  
10 decreases with decreasing  $\Omega_{\text{arag}}$  (McCulloch et al., 2012). The incompatible relationship of  
11 higher  $\text{pH}_{\text{sw}}$  and decreased coral growth suggests that the effects of large flood events on  
12 lowering  $\Omega_{\text{arag}}$  and degrading water quality (e.g. increased shading, turbidity, sedimentation,  
13 or competition for carbon by up-regulated photosynthetic activity of zooxanthellae) are the  
14 dominant cause of reduced coral growth. This study demonstrates the value of coral  $\delta^{11}\text{B}$  as a  
15 paleo-proxy for reconstructing past  $\text{pH}_{\text{sw}}$  changes, as well as the importance of disentangling  
16 the effects of changing local water quality from ocean acidification and global warming,  
17 which is not only relevant to the inner-shelf region of the GBR but other coral systems  
18 worldwide.

19

## 20 **Acknowledgements**

21 The authors are grateful for financial support from by the Australian Research Council Centre  
22 of Excellence for Coral Reef Studies to M.Mc. and J.P.D. M.Mc. was also supported by a  
23 Western Australian Premier's Fellowship and an ARC Laureate Fellowship. J.P.D. was also  
24 supported by a PhD scholarship from the Research School of Earth Science, Australian  
25 National University. The research was completed while J.P.D was holding a Research  
26 Associate position at UWA funded by NERP Tropical Ecosystems Hub Project 1.3 awarded  
27 to M.Mc. We thank Stephen Lewis (James Cook University) who collected (2007) and  
28 assisted (2009) with the collection of water samples and kindly provided the salinity data for  
29 water samples. G. Mortimer provided support for the  $\delta^{11}\text{B}$  measurements at ANU. We thank  
30 J. Falter, S.A Aciego, and one anonymous referee for their constructive comments on the  
31 manuscript.

32

## 1 **References**

- 2 Al-Horani, F. A., Al-Moghrabi, S. M., and de Beer, D.: The mechanism of calcification and  
3 its relation to photosynthesis and respiration in the scleractinian coral *Galaxea fascicularis*,  
4 *Mar Biol*, 142, 419-426, DOI 10.1007/s00227-002-0981-8, 2003.
- 5 Albright, R., Langdon, C., and Anthony, K. R. N.: Dynamics of seawater carbonate  
6 chemistry, production, and calcification of a coral reef flat, central Great Barrier Reef,  
7 *Biogeosciences*, 10, 6747-6758, 10.5194/bg-10-6747-2013, 2013.
- 8 Allemand, D., Tambutt, E. E., Girard, J. P., and Jaubert, J.: Organic matrix synthesis in the  
9 scleractinian coral *Stylophora pistillata*: role in biomineralization and potential target of the  
10 organotin tributyltin, *J Exp Biol*, 201 (Pt 13), 2001-2009, 1998.
- 11 Allemand, D., Ferrier-Pages, C., Furla, P., Houlbreque, F., Puverel, S., Reynaud, S.,  
12 Tambutte, E., Tambutte, S., and Zoccola, D.: Biomineralisation in reef-building corals: from  
13 molecular mechanisms to environmental control, *C R Palevol*, 3, 453-467, DOI  
14 10.1016/j.crpv.2004.07.011, 2004.
- 15 Andersson, A. J., Mackenzie, F. T., and Lerman, A.: Coastal ocean and carbonate systems in  
16 the high CO<sub>2</sub> world of the anthropocene, *Am J Sci*, 305, 875 - 918, 2005.
- 17 Barth, S.: <sup>11</sup>B/<sup>10</sup>B variations of dissolved boron in a freshwater-seawater mixing plume (Elbe  
18 Estuary, North Sea), *Mar Chem*, 62, 1-14, 1998.
- 19 Bates, N. R., Amat, A., and Andersson, A. J.: Feedbacks and responses of coral calcification  
20 on the Bermuda reef system to seasonal changes in biological processes and ocean  
21 acidification, *Biogeosciences*, 7, 2509-2530, 10.5194/bg-7-2509-2010, 2010.
- 22 Bates, N. R., Best, M. H. P., Neely, K., Garley, R., Dickson, A. G., and Johnson, R. J.:  
23 Detecting anthropogenic carbon dioxide uptake and ocean acidification in the North Atlantic  
24 Ocean, *Biogeosciences*, 9, 2509-2522, 10.5194/bg-9-2509-2012, 2012.
- 25 Belperio, A.: The combined use of wash loads and bed material load rating curves for the  
26 calculation of total load: an example from the Burdekin River, Australia, *Catena*, 6, 317 -  
27 329, 1979.
- 28 Brodie, J., Fabricius, K., De'ath, G., and Okaji, K.: Are increased nutrient inputs responsible  
29 for more outbreaks of crown-of-thorns starfish? An appraisal of the evidence, *Mar Pollut*  
30 *Bull*, 51, 266-278, 10.1016/j.marpolbul.2004.10.035, 2005.
- 31 Brodie, J., Schroeder, T., Rohde, K., Faithful, J., Masters, B., Dekker, A., Brando, V., and  
32 Maughan, M.: Dispersal of suspended sediments and nutrients in the Great Barrier Reef  
33 lagoon during river-discharge events: conclusions from satellite remote sensing and  
34 concurrent flood-plume sampling, *Mar Freshwater Res*, 61, 651 - 664, 2010a.
- 35 Brodie, J., Wolanski, E., Lewis, S., and Bainbridge, Z.: An assessment of residence times of  
36 land-sourced contaminants in the Great Barrier Reef lagoon and the implications for  
37 management and reef recovery, *Mar Pollut Bull*, 65, 267-279,  
38 10.1016/j.marpolbul.2011.12.011, 2012.
- 39 Brodie, J. E., De'ath, G., Devlin, M., Furnas, M., and Wright, M.: Spatial and temporal  
40 patterns of near-surface chlorophyll a in the Great Barrier Reef lagoon, *Mar Freshwater Res*,  
41 58, 342-353, 2007.

- 1 Brodie, J. E., Devlin, M., Haynes, D., and Waterhouse, J.: Assessment of the eutrophication  
2 status of the Great Barrier Reef lagoon (Australia), *Biogeochemistry*, 106, 281-302,  
3 10.1007/s10533-010-9542-2, 2010b.
- 4 Cantin, N. E., and Lough, J. M.: Surviving coral bleaching events: *Porites* growth anomalies  
5 on the Great Barrier Reef, *PloS ONE*, 9, e88720, 10.1371/journal.pone.0088720, 2014.
- 6 Cooper, T. F., De'Ath, G., Fabricius, K. E., and Lough, J. M.: Declining coral calcification in  
7 massive *Porites* in two nearshore regions of the northern Great Barrier Reef, *Glob Change*  
8 *Biol*, 14, 529-538, 10.1111/j.1365-2486.2007.01520.x, 2008.
- 9 D'Olivo, J. P., McCulloch, M. T., and Judd, K.: Long-term records of coral calcification  
10 across the central Great Barrier Reef: assessing the impacts of river runoff and climate  
11 change, *Coral Reefs*, 10.1007/s00338-013-1071-8, 2013.
- 12 De'ath, G., Lough, J. M., and Fabricius, K. E.: Declining coral calcification on the Great  
13 Barrier Reef, *Science*, 323, 116-119, 10.1126/science.1165283, 2009.
- 14 De'ath, G., and Fabricius, K.: Water quality as a regional driver of coral biodiversity and  
15 macroalgae on the Great Barrier Reef, *Ecol Appl*, 20, 840-850, 2010.
- 16 Devlin, M. J., and Brodie, J.: Terrestrial discharge into the Great Barrier Reef Lagoon:  
17 nutrient behavior in coastal waters, *Mar Pollut Bull*, 51, 9-22,  
18 10.1016/j.marpolbul.2004.10.037, 2005.
- 19 Dickson, A. G., and Millero, F. J.: A Comparison of the Equilibrium-Constants for the  
20 Dissociation of Carbonic-Acid in Seawater Media, *Deep-Sea Res*, 34, 1733-1743, 1987.
- 21 Dickson, A. G.: Thermodynamics of the dissociation of boric acid in synthetic seawater from  
22 273.15 to 318.15 K, *Deep-Sea Res*, 37, 755-766, 1990.
- 23 Doney, S. C., Fabry, V. J., Feely, R. A., and Kleypas, J. A.: Ocean acidification: the other  
24 CO<sub>2</sub> problem, *Ann Rev Mar Sci*, 1, 169-192, 10.1146/annurev.marine.010908.163834, 2009.
- 25 Dore, J. E., Lukas, R., Sadler, D. W., Church, M. J., and Karl, D. M.: Physical and  
26 biogeochemical modulation of ocean acidification in the central North Pacific, *P Natl Acad*  
27 *Sci USA*, 106, 12235-12240, 10.1073/pnas.0906044106, 2009.
- 28 Drupp, P., De Carlo, E. H., Mackenzie, F. T., Bienfang, P., and Sabine, C. L.: Nutrient  
29 Inputs, Phytoplankton Response, and CO<sub>2</sub> Variations in a Semi-Enclosed Subtropical  
30 Embayment, Kaneohe Bay, Hawaii, *Aquat Geochem*, 17, 473-498, 10.1007/s10498-010-  
31 9115-y, 2011.
- 32 Duarte, C. M., Hendriks, I. E., Moore, T. S., Olsen, Y. S., Steckbauer, A., Ramajo, L.,  
33 Carstensen, J., Trotter, J. A., and McCulloch, M.: Is Ocean Acidification an Open-Ocean  
34 Syndrome? Understanding Anthropogenic Impacts on Seawater pH, *Estuar Coasts*, 36, 221-  
35 236, 10.1007/s12237-013-9594-3, 2013.
- 36 Fabricius, K. E., Logan, M., Weeks, S., and Brodie, J.: The effects of river run-off on water  
37 clarity across the central Great Barrier Reef, *Mar Pollut Bull*,  
38 10.1016/j.marpolbul.2014.05.012, 2014.
- 39 Falter, J. L., Lowe, R. J., Zhang, Z., and McCulloch, M.: Physical and biological controls on  
40 the carbonate chemistry of coral reef waters: effects of metabolism, wave forcing, sea level,  
41 and geomorphology, *PloS ONE*, 8, e53303, 10.1371/journal.pone.0053303, 2013.
- 42 Foster, G. L., Pogge von Strandmann, P. A. E., and Rae, J. W. B.: Boron and magnesium  
43 isotopic composition of seawater, *Geochem Geophys Geosys*, 11, 10.1029/2010gc003201,  
44 2010.

- 1 Foster, G. L., Hönlisch, B., Paris, G., Dwyer, G. S., Rae, J. W. B., Elliott, T., Gaillardet, J.,  
2 Hemming, N. G., Louvat, P., and Vengosh, A.: Interlaboratory comparison of boron isotope  
3 analyses of boric acid, seawater and marine CaCO<sub>3</sub> by MC-ICPMS and NTIMS, *Chemical*  
4 *Geology*, 358, 1-14, 10.1016/j.chemgeo.2013.08.027, 2013.
- 5 Frithsen, J. B., Keller, A. A., and Pilson, M. E. Q.: Effects of inorganic nutrient additions in  
6 coastal areas: a mesocosm experiment; data report, Marine Ecosystems Research Laboratory,  
7 Graduate School of Oceanography, University of Rhode Island, 1985.
- 8 Furnas, M.: Catchments and corals: terrestrial runoff to the Great Barrier Reef, Australian  
9 Institute of Marine Science and Reef CRC, Townsville, Australia, 2003.
- 10 Furnas, M., Mitchell, A., Skuza, M., and Brodie, J.: In the other 90%: phytoplankton  
11 responses to enhanced nutrient availability in the Great Barrier Reef Lagoon, *Marine*  
12 *pollution bulletin*, 51, 253-265, 10.1016/j.marpolbul.2004.11.010, 2005.
- 13 Furnas, M., Alongi, D., McKinnon, D., Trott, L., and Skuza, M.: Regional-scale nitrogen and  
14 phosphorus budgets for the northern (14°S) and central (17°S) Great Barrier Reef shelf  
15 ecosystem, *Continental Shelf Research*, 31, 1967-1990, 10.1016/j.csr.2011.09.007, 2011.
- 16 Gagliano, M., McCormick, M. I., Moore, J. A., and Depczynski, M.: The basics of  
17 acidification: baseline variability of pH on Australian coral reefs, *Mar Biol*, 157, 1849-1856,  
18 10.1007/s00227-010-1456-y, 2010.
- 19 Gattuso, J.-P., Frankignoulle, M., and Smith, S. V.: Measurement of community metabolism  
20 and significance in the coral reef CO<sub>2</sub> source-sink debate, *P Natl Acad Sci USA*, 96, 13017-  
21 13022, 1999.
- 22 Hallock, P., and Schlager, W.: Nutrient excess and the demise of coral reefs and carbonate  
23 platforms, *PALAIOS*, 1, 389-398, 1986.
- 24 Hemming, N. G., and Hanson, G. N.: Boron isotopic composition and concentration in  
25 modern marine carbonates, *Geochim Cosmochim Acta*, 56, 537-543, 1992.
- 26 Hinga, K. R.: Effects of pH on coastal marine phytoplankton, *Mar Ecol-Prog Ser*, 238, 281-  
27 300, 2002.
- 28 Hönlisch, B., Hemming, N. G., Grottoli, A. G., Amat, A., Hanson, G. N., and Buma, J.:  
29 Assessing scleractinian corals as recorders for paleo-pH: Empirical calibration and vital  
30 effects, *Geochim Cosmochim Acta*, 68, 3675-3685, DOI 10.1016/j.gca.2004.03.0026, 2004.
- 31 Jones, P. D., Briffa, K. R., Osborn, T., Lough, J., van Ommen, T. D., Vinther, B. M.,  
32 Luterbacher, J., Wahl, E. R., Zwiers, F. W., Mann, M. E., Schmidt, G. A., Ammann, C. M.,  
33 Buckley, B. M., Cobb, K. M., Esper, J., Goosse, H., Graham, N., Jansen, E., Kiefer, T., Kull,  
34 C., Küttel, E., Mosley-Thompson, E., Overpeck, J. T., Riedwyl, N., Schultz, M., Tudhope, A.  
35 W., Villalba, R., Wanner, H., Wolff, E., and Xoplaki, E.: High-resolution palaeoclimatology  
36 of the last millennium: a review of current status and future prospects, *Holocene*, 19, 3-49,  
37 2009.
- 38 King, B., McAllister, F., Wolanski, E., Done, T., and Spagnol, S.: River plume dynamics in  
39 the central Great Barrier Reef, in: *Oceanographic Processes of Coral reefs: Physical and*  
40 *Biological Links in the Great Barrier Reef*, edited by: Wolanski, E., CRC Press, Boca Raton,  
41 145-160, 2001.
- 42 King, B., McAllister, F., and Done, T.: Modelling the impact of the Burdekin, Herbert, Tully  
43 and Johnstone River plumes on the Central Great Barrier Reef, CRC Reef Research Centre,  
44 Townsville, 2002.

- 1 Kleypas, J. A.: Geochemical Consequences of Increased Atmospheric Carbon Dioxide on  
2 Coral Reefs, *Science*, 284, 118-120, 10.1126/science.284.5411.118, 1999.
- 3 Klochko, K., Kaufman, A. J., Yao, W., Byrne, R. H., and Tossell, J. A.: Experimental  
4 measurement of boron isotope fractionation in seawater, *Earth Planet Sc Lett*, 248, 276-285,  
5 10.1016/j.epsl.2006.05.034, 2006.
- 6 Krief, S., Hendy, E. J., Fine, M., Yam, R., Meibom, A., Foster, G. L., and Shemesh, A.:  
7 Physiological and isotopic responses of scleractinian corals to ocean acidification, *Geochim  
8 Cosmochim Ac*, 74, 4988-5001, 10.1016/j.gca.2010.05.023, 2010.
- 9 Lewis, S. E., Shields, G. A., Kamber, B. S., and Lough, J. M.: A multi-trace element coral  
10 record of land-use changes in the Burdekin River catchment, NE Australia, *Palaeogeogr  
11 Palaeocl*, 246, 471-487, 10.1016/j.palaeo.2006.10.021, 2007.
- 12 Liu, Y., Liu, W., Peng, Z., Xiao, Y., Wei, G., Sun, W., He, J., Liu, G., and Chou, C.-L.:  
13 Instability of seawater pH in the South China Sea during the mid-late Holocene: Evidence  
14 from boron isotopic composition of corals, *Geochim Cosmochim Ac*, 73, 1264-1272,  
15 10.1016/j.gca.2008.11.034, 2009.
- 16 Lough, J.: Climate variability and change on the Great Barrier Reef, in: *Oceanographic  
17 Processes of Coral Reefs: Physical and Biological Links in the Great Barrier Reef*, edited by:  
18 Wolanski, E., CRC Press, Boca Raton, Florida, 269-300, 2001.
- 19 Lough, J. M.: A strategy to improve the contribution of coral data to high-resolution  
20 paleoclimatology, *Palaeogeogr Palaeocl*, 204, 115-143, 10.1016/s0031-0182(03)00727-2,  
21 2004.
- 22 Lough, J. M.: Tropical river flow and rainfall reconstructions from coral luminescence: Great  
23 Barrier Reef, Australia, *Paleoceanography*, 22, 10.1029/2006pa001377, 2007.
- 24 Lough, J. M.: Coral calcification from skeletal records revisited, *Mar Ecol-Prog Ser*, 373,  
25 257-264, 10.3354/meps07398, 2008.
- 26 Lough, J. M.: Measured coral luminescence as a freshwater proxy: comparison with visual  
27 indices and a potential age artefact, *Coral Reefs*, 30, 169-182, DOI 10.1007/s00338-010-  
28 0688-0, 2011.
- 29 McCulloch, M., Falter, J., Trotter, J., and Montagna, P.: Coral resilience to ocean  
30 acidification and global warming through pH up-regulation, *Nat Clim Change*, 2, 623-627,  
31 10.1038/nclimate1473, 2012.
- 32 McCulloch, M. T., Fallon, S., Wyndham, T., Hendy, E., Lough, J. M., and Barnes, D. J.:  
33 Coral record of increased sediment flux to the inner Great Barrier Reef since European  
34 settlement, *Nature*, 421, 727-730, Doi 10.1038/Nature01361, 2003.
- 35 McCulloch, M. T., Holcomb, M., Rankenburg, K., and Trotter, J. A.: Rapid, high-precision  
36 measurements of boron isotopic compositions in marine carbonates, *Rapid Commun Mass  
37 Spectrom*, 28, 2704-2712, 10.1002/rcm.7065, 2014.
- 38 Merzbach, C., Culberson, C. H., Hawley, J. E., and Pytkowicz, R. M.: Measurement of the  
39 apparent dissociation constants of carbonic acid in seawater at atmospheric pressure, *Limnol  
40 Oceanogr*, 18, 897-907, 1973.
- 41 Mitchell, A. W., and Bramley, R. G. V.: Export of nutrients and suspended sediment from the  
42 Herbert river catchment during a flood event associated with cyclone Sadie, *Cyclone Sadie  
43 Flood Plumes in the GBR lagoon: Composition and Consequences*, Workshop series. Great  
44 Barrier Reef Marine Park Authority. No. 22. 1997, 1997,

- 1 Palmer, M. R., Spivack, A. J., and Edmond, J. M.: Temperature and pH controls over isotopic  
2 fractionation during adsorption of boron on marine clay, *Geochim Cosmochim Acta*, 51, 2139-  
3 2323, 1987.
- 4 Pelejero, C., Calvo, E., McCulloch, M. T., Marshall, J. F., Gagan, M. K., Lough, J. M., and  
5 Opdyke, B. N.: Preindustrial to modern interdecadal variability in coral reef pH, *Science*,  
6 309, 2204-2207, 10.1126/science.1113692, 2005.
- 7 Philipp, E., and Fabricius, K.: Photophysiological stress in scleractinian corals in response to  
8 short-term sedimentation, *J Exp Mar Biol Ecol*, 287, 57-78, 2003.
- 9 Reynaud, S., Hemming, N. G., Juillet-Leclerc, A., and Gattuso, J. P.: Effect of  $\rho\text{CO}_2$  and  
10 temperature on the boron isotopic composition of the zooxanthellate coral *Acropora* sp, *Coral*  
11 *Reefs*, 23, 539-546, 10.1007/s00338-004-0399-5, 2004.
- 12 Riegl, B., and Branch, G. M.: Effects of sediment on the energy budgets of four scleractinian  
13 (Bourne 1900) and five alcyonacean (Lamouroux 1816) corals, *J Exp Mar Biol Ecol*, 186,  
14 259-275, 1995.
- 15 Salisbury, J., Green, M., Hunt, C., and Campbell, J.: Coastal acidification by rivers: a threat  
16 to shellfish?, *EOS*, 89, 513-528, 2008.
- 17 Santana-Casiano, J. M., González-Dávila, M., Rueda, M.-J., Llinás, O., and González-Dávila,  
18 E.-F.: The interannual variability of oceanic  $\text{CO}_2$  parameters in the northeast Atlantic  
19 subtropical gyre at the ESTOC site, *Global Biogeochem Cy*, 21, n/a-n/a,  
20 10.1029/2006gb002788, 2007.
- 21 Shinjo, R., Asami, R., Huang, K.-F., You, C.-F., and Iryu, Y.: Ocean acidification trend in the  
22 tropical North Pacific since the mid-20th century reconstructed from a coral archive, *Mar*  
23 *Geol*, 10.1016/j.margeo.2013.06.002, 2013.
- 24 Simpson, J. J., and Zirino, A.: Biological-control of pH in the Peruvian coastal upwelling  
25 area, *Deep-Sea Res*, 27, 733-744, 1980.
- 26 Spivack, A. J., and Edmond, J. M.: Determination of boron isotope ratios by thermal  
27 ionization mass-spectrometry of the dicesium metaborate cation, *Anal Chem*, 58, 31-35,  
28 1986.
- 29 Sweatman, H., Delean, S., and Syms, C.: Assessing loss of coral cover on Australia's Great  
30 Barrier Reef over two decades, with implications for longer-term trends, *Coral Reefs*, 30,  
31 521-531, 10.1007/s00338-010-0715-1, 2011.
- 32 Tambutte, E., Allemand, D., Mueller, E., and Jaubert, J.: A compartmental approach to the  
33 mechanism of calcification in hermatypic corals, *J Exp Biol*, 199, 1029-1041, 1996.
- 34 Telesnicki, G. J., and Goldberg, W. M.: Effects of turbidity on the photosynthesis and  
35 respiration of two south Florida Reef coral species, *B Mar Sci*, 57, 527-539, 1995.
- 36 Trotter, J., Montagna, P., McCulloch, M., Silenzi, S., Reynaud, S., Mortimer, G., Martin, S.,  
37 Ferrier-Pagès, C., Gattuso, J.-P., and Rodolfo-Metalpa, R.: Quantifying the pH 'vital effect'  
38 in the temperate zooxanthellate coral *Cladocora caespitosa*: Validation of the boron seawater  
39 pH proxy, *Earth Planet Sc Lett*, 303, 163-173, 10.1016/j.epsl.2011.01.030, 2011.
- 40 Uthicke, S., Furnas, M., and Lonborg, C.: Coral reefs on the edge? Carbon chemistry on  
41 inshore reefs of the great barrier reef, *PloS one*, 9, e109092, 10.1371/journal.pone.0109092,  
42 2014.

- 1 Vengosh, A., Kolodny, Y., Starinsky, A., Chivas, A. R., and McCulloch, M. T.:  
2 Coprecipitation and Isotopic Fractionation of Boron in Modern Biogenic Carbonates,  
3 *Geochim Cosmochim Acta*, 55, 2901-2910, 1991.
- 4 Venn, A., Tambutte, E., Holcomb, M., Allemand, D., and Tambutte, S.: Live tissue imaging  
5 shows reef corals elevate pH under their calcifying tissue relative to seawater, *PloS ONE*, 6,  
6 e20013, 10.1371/journal.pone.0020013, 2011.
- 7 Wang, B. S., You, C. F., Huang, K. F., Wu, S. F., Aggarwal, S. K., Chung, C. H., and Lin, P.  
8 Y.: Direct separation of boron from Na- and Ca-rich matrices by sublimation for stable  
9 isotope measurement by MC-ICP-MS, *Talanta*, 82, 1378-1384,  
10 10.1016/j.talanta.2010.07.010, 2010.
- 11 Walker, T.: Seasonal Salinity Variations in Cleveland Bay, Northern Queensland, *Aust J Mar*  
12 *Fresh Res*, 32, 143-149, 1981.
- 13 Wei, G., McCulloch, M. T., Mortimer, G., Deng, W., and Xie, L.: Evidence for ocean  
14 acidification in the Great Barrier Reef of Australia, *Geochim Cosmochim Acta*, 73, 2332-2346,  
15 10.1016/j.gca.2009.02.009, 2009.
- 16 Wolanski, E., and Jones, M.: Physical properties of the Great Barrier Reef lagoon waters near  
17 Townsville. I effects of Burdekin River floods, *Aust J Mar Fresh Res*, 32, 305-319, 1981.
- 18 Xiao, Y., Liao, B., Wang, Z., Wei, H., and Zhao, Z.: Isotopic composition of dissolved boron  
19 and its geochemical behavior in a freshwater-seawater mixture at the estuary of the  
20 Changjiang (Yangtze) River, *Chinese J Geochem*, 26, 105-113, 2007.
- 21

1 Table 1. Periods covered by coral core samples analysed.

<b>Region</b>	<b>Reef</b>	<b>Core</b>	<b>Years</b>
Inner-shelf	Havannah Is.	HAV06A	1966-2005
		HAV09_3	1940-2009
	Pandora	PAN02	1963-2002
Mid-shelf	Rib	RIB09_3	1964-2009
	17-065	1709_6	1973-2009

2

3



1 Table 2. Average values and variability (2 SD) for coral  $\delta^{11}\text{B}_{\text{carb}}$ ,  $\text{pH}_{\text{cf}}$ , and reconstructed  
 2  $\text{pH}_{\text{sw}}$  calculated over the common period of 1973-2002. The reconstructed  $\text{pH}_{\text{sw}}$  values were  
 3 estimated using Eq. (2) to correct for the pH offset at the site of calcification. Slopes were  
 4 obtained from the linear regression of the full length of each core (see Table 1) and are used  
 5 to indicate the annual rate of change for the reconstructed  $\text{pH}_{\text{sw}}$  records. The uncertainty for  
 6 the slopes is based on the external reproducibility for the standard.

		$\delta^{11}\text{B}_{\text{carb}}$	$\text{pH}_{\text{cf}}$	$\text{pH}_{\text{sw}}$	
<b>Core</b>		<b>Average</b>	<b>Average</b>	<b>Average</b>	<b>Slope (pH unit yr<sup>-1</sup>)</b>
Inner-shelf	HAV06A	25.17±0.57	8.58±0.04	8.19±0.11	-0.0020±0.0030
	HAV09_3	24.15±0.50	8.54±0.03	8.08±0.10	-0.0023±0.0011
	PAN02	24.54±0.66	8.54±0.04	8.07±0.13	-0.0008±0.0038
Mid-shelf	RIB09_3	24.20±0.44	8.51±0.03	8.00±0.09	-0.0023±0.0020
	1709_6	23.60±0.37	8.48±0.02	7.88±0.07	-0.0013±0.0021

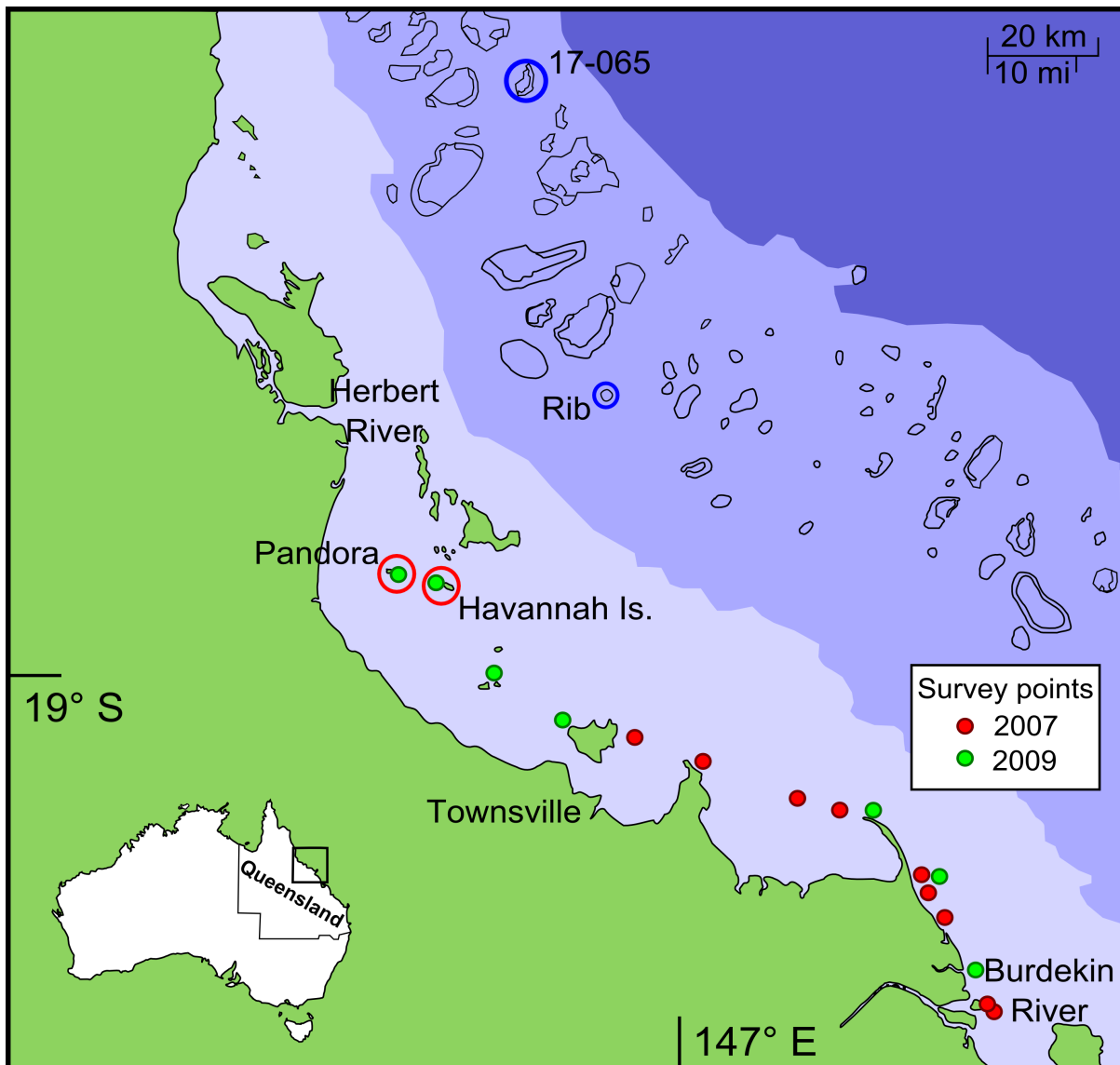
7

1 Table 3. Pearson correlation coefficients (r) and corresponding p-values for correlations of  
 2 annual composite coral  $\delta^{11}\text{B}_{\text{carb}}$  records from the inner-shelf (1964 to 2005) and mid-shelf  
 3 (1973 to 2009) with Burdekin River runoff, SST from HadISST1, and coral linear extension  
 4 rates for the corresponding region taken from D’Olivo et al. (2013).

	River runoff (log ML)		SST (°C)		Lin ext (cm yr <sup>-1</sup> )	
	r	p-value	r	p-value	r	p-value
$\delta^{11}\text{B}_{\text{carb}}$ inner-shelf (n=42)	0.565	0.0001	-0.387	0.0103	-0.418	0.0053
$\delta^{11}\text{B}_{\text{carb}}$ mid-shelf (n=37)	0.147	0.3860	-0.420	0.0096	-0.302	0.0733

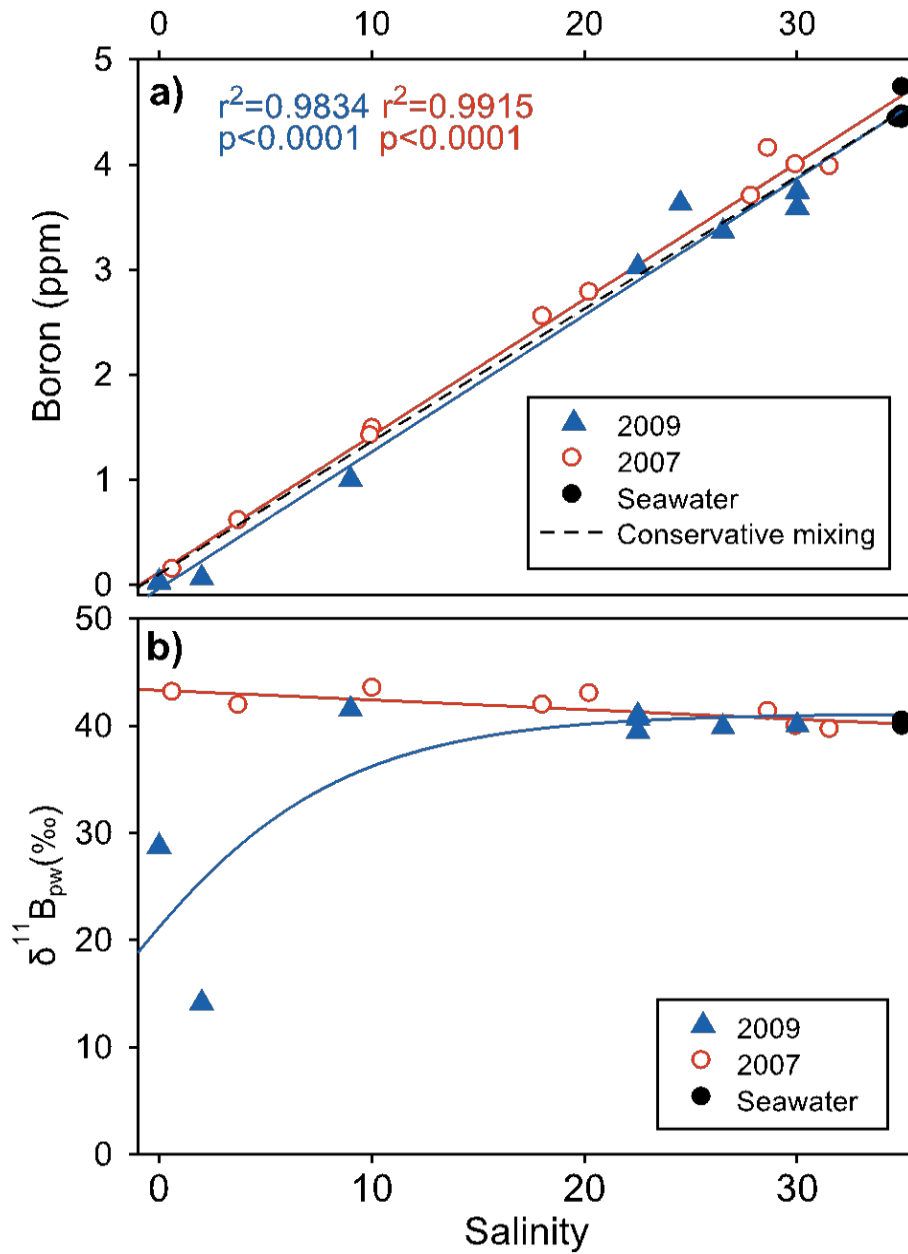
5  
6

1  
2



3  
4 Figure 1. Map of the central area of the GBR showing locations of water sample and coral  
5 core collection sites: Pandora Reef and Havannah Island in the inner-shelf; Rib Reef and 17-  
6 065 Reef in the mid-shelf region; water sample collection sites during the flood events of  
7 2007 and 2009.

8

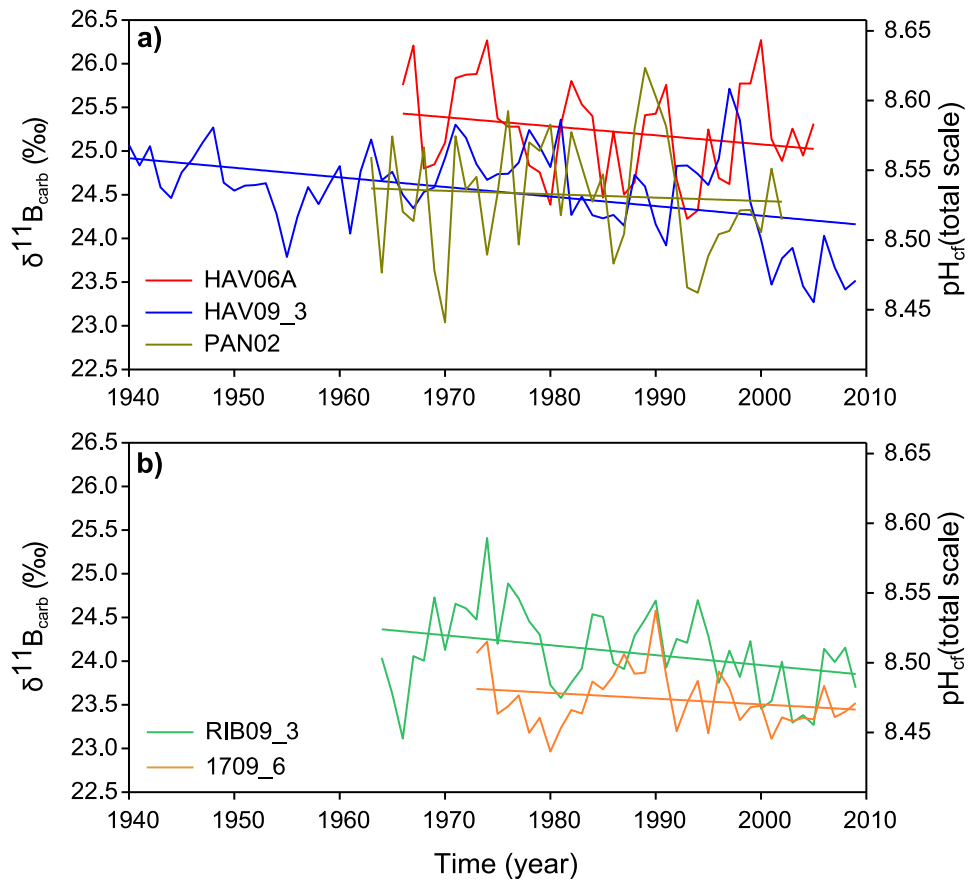


1

2 Figure 2. (a) Boron concentration plotted against salinity of waters from the flood events of  
 3 2007 and 2009. A linear regression through the data is compared to the theoretical  
 4 conservative mixing relationship based on a seawater end-member with 4.52 mg B/l at S =  
 5 35. (b) Boron isotope composition of waters along salinity transects from the 2007 and 2009  
 6 flood events.

7

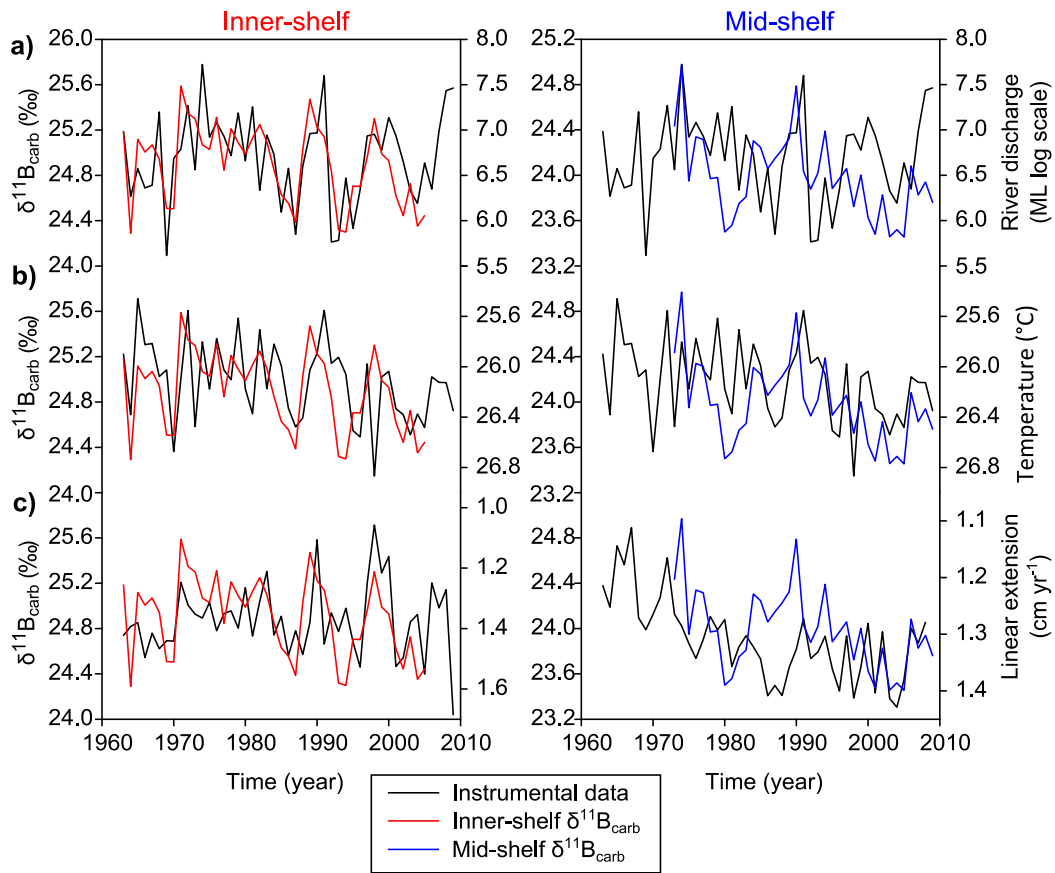
1



2

3 Figure 3. Annual time-series and linear regressions for  $\delta^{11}\text{B}_{\text{carb}}$  values and  
4 corresponding  $\text{pH}_{\text{cf}}$  of coral cores from (a) the inner-shelf reefs of Havannah Island and  
5 Pandora Reef, and (b) the mid-shelf reefs of Rib Reef and 17-065.

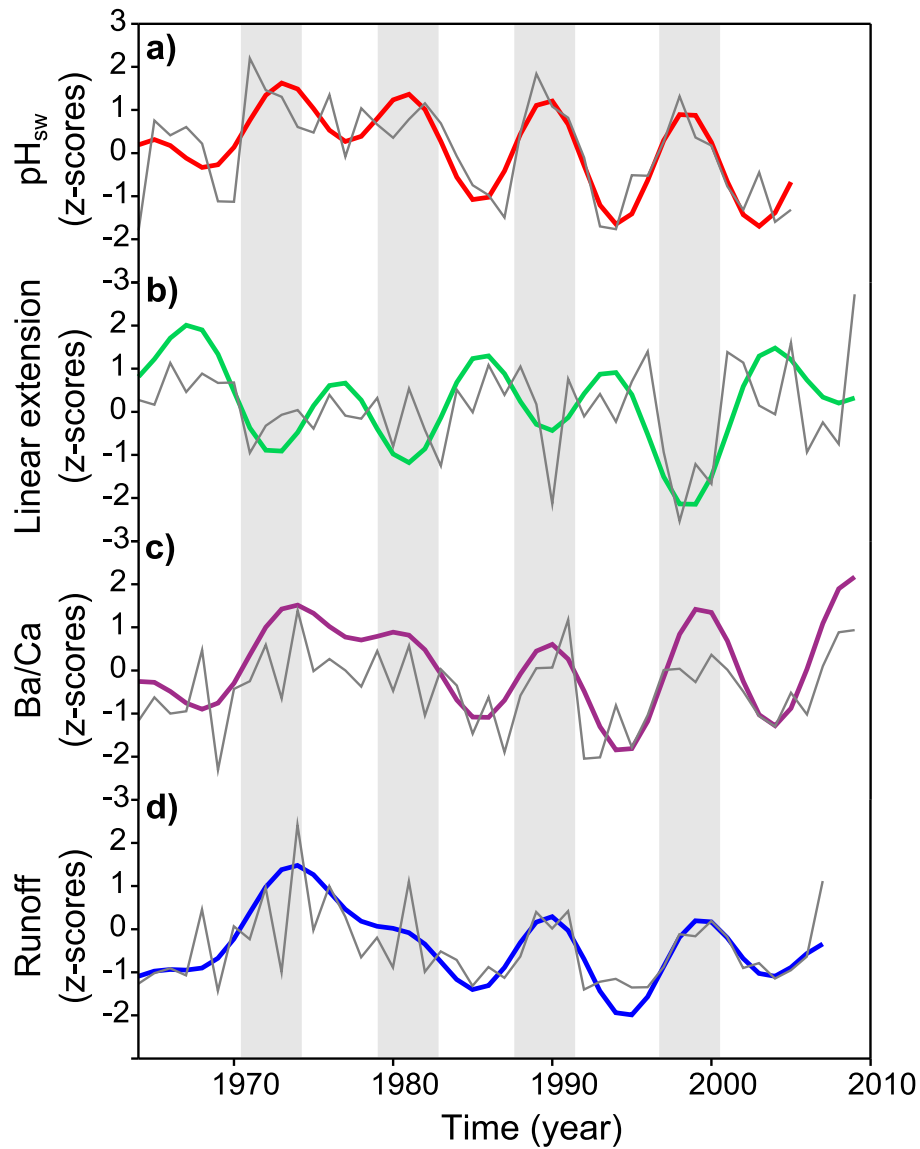
1



2

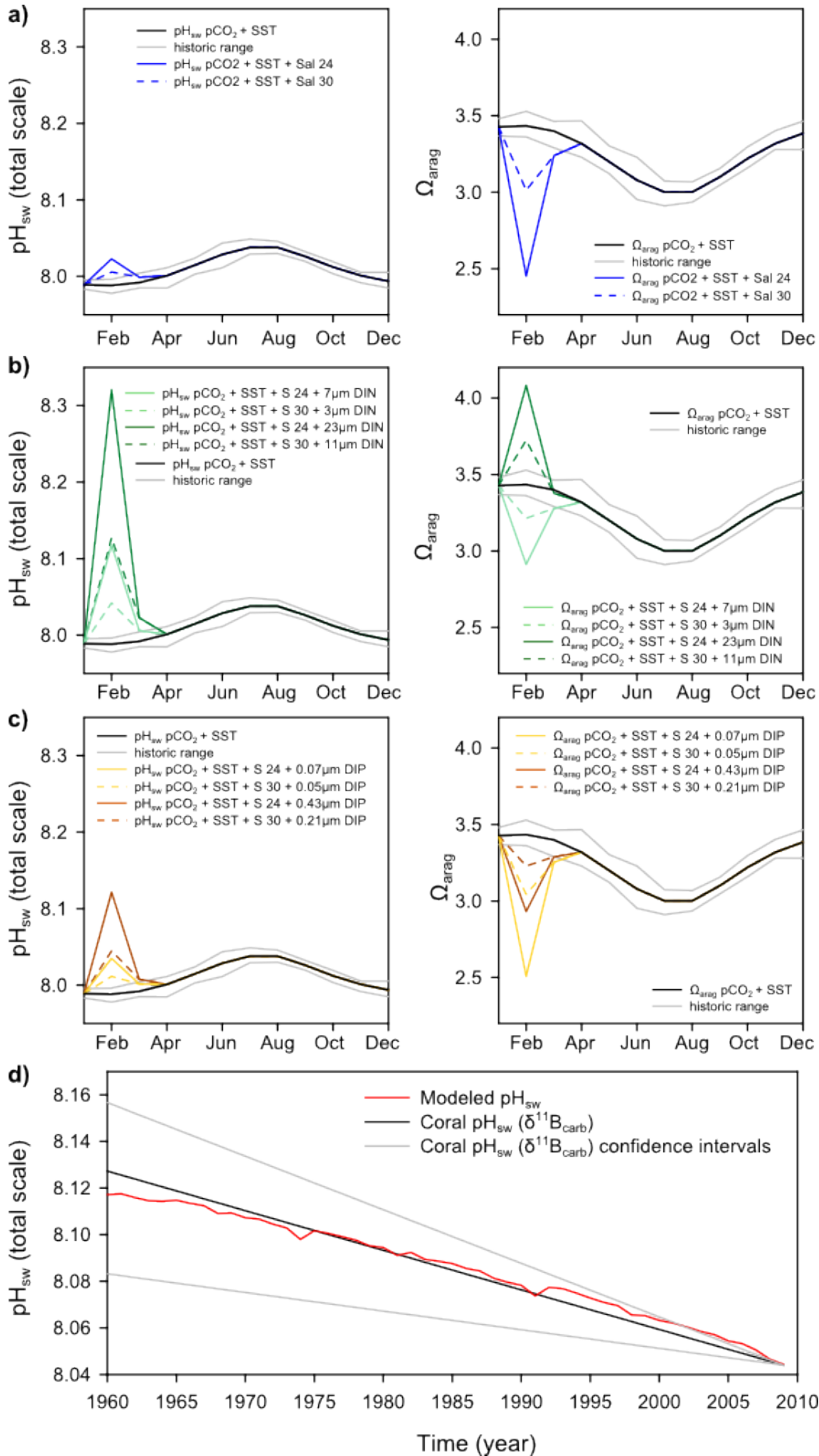
3 Figure 4. Annual composite  $\delta^{11}\text{B}_{\text{carb}}$  records for the inner-shelf corals and mid-shelf corals  
4 compared to annual discharge from the Burdekin River (panel a), SST from HadISST1 (panel  
5 b), and coral linear extension rates from D'Olivo et al. (2013) for the corresponding inner-  
6 shelf or mid-shelf regions (panel c). Note that the temperature and linear extension axis has  
7 been reversed to facilitate comparisons.

8



1  
2  
3  
4  
5  
6  
7

Figure 5. Normalized annual (grey) and smoothed (coloured 8-year low band pass filter) time-series for (a) the inner-shelf composite reconstructed  $\text{pH}_{\text{sw}}$  obtained from  $\delta^{11}\text{B}_{\text{carb}}$  coral records, (b) averaged linear extension of inner-shelf in the central GBR (D’Olivo et al., 2013), terrestrial influx indicated by (c) discharge from the Burdekin River, and (d) coral Ba/Ca data from Pandora and Havannah Is (McCulloch et al., 2003).





1 Figure 6. (a) Estimated seasonal  $\text{pH}_{\text{sw}}$  and  $\Omega_{\text{arag}}$  changes based on in situ SST (AIMS;  
2 2011) with an average  $\text{pCO}_2$  of 431 ppm and a seasonal variation of 60 ppm (Uthicke et  
3 al., 2014). Seawater pH values were estimated considering a seawater end-member  
4 with summer TA of  $2270 \text{ mmol kgsw}^{-1}$  and winter TA of  $2256 \text{ mmol kgsw}^{-1}$  (Uthicke  
5 et al., 2014), DIC changes were estimated from TA and  $\text{pCO}_2$ . The grey lines define the  
6 range of historic maximum and minimum SST values for any given month. Changes in  
7  $\text{pH}_{\text{sw}}$  and  $\Omega_{\text{arag}}$  resulting from a hypothetical flood events characterized by a decrease in  
8 salinity from 35 to values of 30 and 24 in February, and increasing to 33 in March are  
9 shown. For flood conditions the river water end-member was estimated considering TA  
10 of  $787.7 \text{ mmol kgsw}^{-1}$  and DIC of  $811.1 \text{ mmol kgsw}^{-1}$  (DERM; 2014). (b) Estimated  
11 seasonal  $\text{pH}_{\text{sw}}$  and  $\Omega_{\text{arag}}$  changes as in (a), including DIC changes associated to the  $\text{CO}_2$   
12 drawdown due to enhanced phytoplankton production during flood events based on  
13 DIN river inputs of 20 and  $70 \mu\text{M}$  in February and assuming conservative dilution.  
14 Nutrient inputs are estimated to reduce by half in March and back to seawater levels by  
15 April. (c) Estimated seasonal  $\text{pH}_{\text{sw}}$  and  $\Omega_{\text{arag}}$  changes as in (b) considering DIP river  
16 inputs of 0.15 and  $1.3 \mu\text{M}$  in February and assuming conservative dilution. (d)  
17 Estimated annual  $\text{pH}_{\text{sw}}$  changes with time based on reconstructed SST (HadISST1),  
18 changes in atmospheric  $\text{CO}_2$  (NOAA), and salinity changes associated with flood  
19 events obtained from the equation in Figure S1. A comparison based on the average  
20  $\text{pH}_{\text{sw}}$  slope obtained from all the coral  $\delta^{11}\text{B}_{\text{carb}}$  data in Table 2 is included. The  
21 minimum and maximum slopes obtained for the corals in Table 2 are included as  
22 confidence intervals. Calculations were made using  $\text{CO}_2\text{SYS}$  with carbonate constants  
23 K1 and K2 from the Merzbach et al. (1973) refit by Dickson and Millero (1987), and  
24 for sulfate from Dickson (1990) with 0 dbar pressure.